Supporting Information for
"Improving Synoptic and Intra-Seasonal Variability in CFSv2 via Stochastic Representation of Organized Convection"

B.B. Goswami[1], B.Khouider[1], R. Phani[2], P. Mukhopadhyay[2], and A. Majda[5]

[1]Department of Mathematics and Statistics, University of Victoria, Victoria, BC, Canada.

[2]Indian Institute of Tropical Meteorology, Pune, India.

[3]Department of Mathematics and Center for Atmosphere and Ocean Sciences, Courant Institute for Mathematical Sciences, New York University, New York, NY, USA and Center for Prototype Climate Models, New York University Abu Dhabi, Abu Dhabi, United Arab Emirates

Contents

Introduction

While elaborate details on the SMCM and its GCM-implementation can be found in *Khouider et al.* [2010] and *Deng et al.* [2015] in particular, some changes had to be made to make it compatible with CFSv2. A brief step-wise description of the implementation of SMCM in the CFSv2 is provided here.

We are providing Fig S1 to complement the Section 3.1 and the Fig 2 to complement the Section 3.2.

S1. Implementation of SMCM in the CFSv2

S1.1 Computation of the Total Heating

The stochastic multicloud model uses 3 prescribed profiles for convective heating, ϕ_c, ϕ_d and ϕ_s, associated with the cumulus congestus cloud (which warms and moistens the lower troposphere and cool the upper troposphere through radiation and detrainment),

Corresponding author: B.B. Goswami, bgoswami@uvic.ca

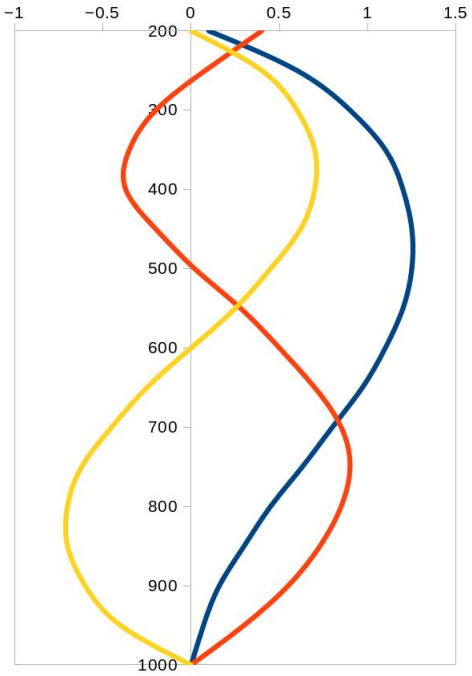

Figure 1. Basis Functions. Cumulus congestus profile in Red; Deep Cumulus profile in Blue; and Stratiform profile in Yellow.

the deep cumulus cloud (which heats up the whole atmospheric column) and the stratiform cloud (which results heating in the upper troposphere), respectively.

While the for original multicloud-model [*Khouider and Majda*, 2006, 2008], simple sine functions were used to set up the basis functions and *Khouider et al.* [2011] used the vertical mode eigenstructure following *Kasahara and Puri* [1981], here we combine observational studies with theory on tropical heating profiles to construct ϕ_c, ϕ_d, ϕ_s. The shape of the deep basis function is designed based on the average heating profile in the Fig-3 of *Stachnik et al.* [2013]. The stratiform basis function is designed following the Stratiform heating profile of the Fig-1 of *Schumacher et al.* [2007]. The congestus structure is designed following *Khouider and Majda* [2006]; however slightly modified to represent the lower level peak (around 700hPa) noted in the convective heating profiles plotted from the CFSR data (not shown here). While constructing ϕ_c, we have also consulted the work of *Schumacher et al.* [2007] (The "Shallow convective" and the "Strongly detraining Cu congestus" profiles in Fig-1).

The total convective heating is computed using the expression :

$$Q_{tot}(z) = H_d\phi_d(z) + H_c\phi_c(z) + H_s\phi_s(z) \tag{1}$$

Where, ϕ_c, ϕ_d and ϕ_s are the three basis functions shown above; and H_c, H_d and H_s are respectively the three associated heating, which are parameterizes using the stochastic area fractions, σ_d, σ_c and σ_s following the dynamical core:

$$H_d = \frac{\sigma_d}{\bar{\sigma_d}} Q_d \tag{2}$$

$$H_c = \frac{\sigma_c}{\bar{\sigma_c}} \alpha_c Q_c \tag{3}$$

$$\frac{\partial H_s}{\partial t} = \frac{T}{\tau_s}\left[\frac{\sigma_s}{\bar{\sigma_s}}\alpha_s H_d - H_s\right] \tag{4}$$

Where, $\bar{\sigma_c}$, $\bar{\sigma_d}$ and $\bar{\sigma_s}$ are the background values of σ_c, σ_d and σ_s respectively.

The cloud area fractions σ_c, σ_d and σ_s describe a Markov jump stochastic process in the form of a multi-dimensional birth-death process whose transition probabilities depend explicitly on the mid tropospheric dryness (MTD), convective available potential energy (CAPE) and convective inhibition (CIN) and vertical velocity (W). The transition rates from one cloud type to the other are same as prescribes in *Deng et al.* [2015], except for the formation of congestus and deep convection from clear sky condition. This change occurs due to the inclusion of CIN and W in the transition rules. The inclusion of CIN and W in the transition rates are driven by the experience gotten during the training of the model. The modified transition rates (formation rates of congestus and deep clouds are highlighted in bold) given as:

Description	Transition Rate	Time Scale (h)
Formation of congestus	$R_{01} = \frac{1}{\tau_{01}}(\Gamma(C_L)\Gamma(D)\frac{(1-\Gamma(W^-))+(1-\Gamma(CIN))}{2}$	32
Decay of congestus	$R_{10} = \frac{1}{\tau_{10}}\Gamma(D)$	2
Conversion of congestus to deep	$R_{12} = \frac{1}{\tau_{12}}\Gamma(C)(1-\Gamma(D))$	0.25
Formation of deep	$R_{02} = \frac{1}{\tau_{02}}(\Gamma(C)(1-\Gamma(D))\frac{(1-\Gamma(W^-))+(1-\Gamma(CIN))}{2}$	12
Conversion of deep to stratiform	$R_{23} = \frac{1}{\tau_{23}}$	0.25
Decay of deep	$R_{20} = \frac{1}{\tau_{20}}(1-\Gamma(C))$	9.5
Decay of stratiform	$R_{30} = \frac{1}{\tau_{30}}$	1

The Gamma functions in the above table are defined as:

$$\Gamma(x) = \begin{cases} (1 - e^{-x}), & \text{if } x > 0 \\ 0, & \text{otherwise} \end{cases}$$

And, W^- denotes the negative part of W given by $\min(W, 0)$.

In Eqn (2-4), the potential for deep (Q_d) and congestus (Q_c) convection is computed, using the following equations,

$$Q_d = \left[\bar{Q_d} + \frac{1}{\tau_q} * \frac{L_v}{C_p} * q_m^{'} + \frac{1}{\tau_c}\left(\theta_{eb}^{'} - \gamma_c \theta_m^{'}\right)\right]^+ \tag{5}$$

$$Q_c = \left[\bar{Q_c} + \frac{1}{\tau_c}\left(\theta_{eb}^{'} - \gamma_c \theta_m^{'}\right)\right]^+ \tag{6}$$

And the resulting downdraft is computed as,

$$D_c = \mu\left[\frac{H_s - H_c}{\bar{Q_c}}\right]^+ \tag{7}$$

Here and elsewhere in the paper X^+ denotes the positive part of the variable X given by $\max(X, 0)$.

To be noted, while computing the downdraft the contribution of the deep heating (H_d) is not considered unlike previous versions of SMCM. This was done in order to address the excessive cooling in the atmosphere faced during the development of the model.

In the equations (5) and (6), $\bar{Q_d}$, $\bar{Q_c}$, $\bar{Q_s}$ are the background potentials for deep, congestus and stratiform convection respectively computed by projecting the background convective heating onto the three basis functions mentioned earlier. τ_q and τ_c are different adjustment time scales. $q_m^{'}$, $\theta_{eb}^{'}$, $\theta_m^{'}$ are expressed as,

$$q_m^{'} = q_m - \bar{q_m} \tag{8}$$

$$\theta_{eb}^{'} = \theta_{eb} - \bar{\theta_{eb}} \tag{9}$$

$$\theta_m^{'} = \theta_m - \bar{\theta_m} \tag{10}$$

which are nothing but the deviations of the middle troposphere moisture, equivalent potential temperature at the planetary boundary layer (PBL) and middle troposphere potential temperature respectively from their background states denoted by the bar-ed notations in the equations (8)-(10).

Earlier theoretical studies with SMCM [*Khouider and Majda*, 2006; *Khouider et al.*, 2010; *Deng et al.*, 2015, and the relevant references therein] and the relevant references therein) all rely on the radiative convective equilibrium (RCE) solution (space-time homogeneous solution) of the governing equations to construct the background to set up the parameterization in Equations (2) to (10). However, such solution is not practical in the context of comprehensive climate model because of existence of various inhomogeneities, like, land-ocean, tropics-mid latitude, etc. To overcome this conundrum we have used climate data to compute surrogates for the RCE solution as time and spatial means for a set of boxes centered over different areas of relatively homogeneous climatology. These different areas (boxes) of relatively homogeneous climatology are shown in Figure 2 overlaid over the shows the long term mean of specific humidity at the surface, in order to provide a rationale behind choosing these boxes. We have plotted other thermo-dynamical fields as well (not shown here), before deciding these boxes. Noteworthy, we have smoothed each background fields before inputting it to CFSsmcm. For an example of a background field, middle level specific humidity is shown in Figure 3.

S1.2 Prescribed vertical profiles of heating/cooling and moistening/drying

The surface precipitation is computed as below:

$$P = \int_0^H Q_{tot}(z) * Q_2(z)\ dz \tag{11}$$

The introduction of the structure function $Q_2(z)$ is a new feature of this current version of SMCM. The shape of $Q_2(z)$ resembles the Yanai moisture sink profile. In earlier versions SMCM, the moisture sink was computed considering the whole atmospheric column as one.

Evaporation is given by,

$$E(z) = \left(\delta_m(z)\frac{D_c}{H}\right) \triangle_m \theta_e \tag{12}$$

Where, $\triangle_m = X_b - X_m$, the suffixes b and m indicate the PBL and middle troposphere values of any variable X. H is the height of the atmosphere (in meters). The form of the function $\delta_m(z)$ is defined as :

$$\delta_m(z) = \begin{cases} 2\exp\left(-\alpha_m \frac{|P(z)-P_{MID}|}{P_{BOT}-P_{TOP}}\right), & \text{if } z \geq h \\ 0, & \text{if } z < h \end{cases}$$

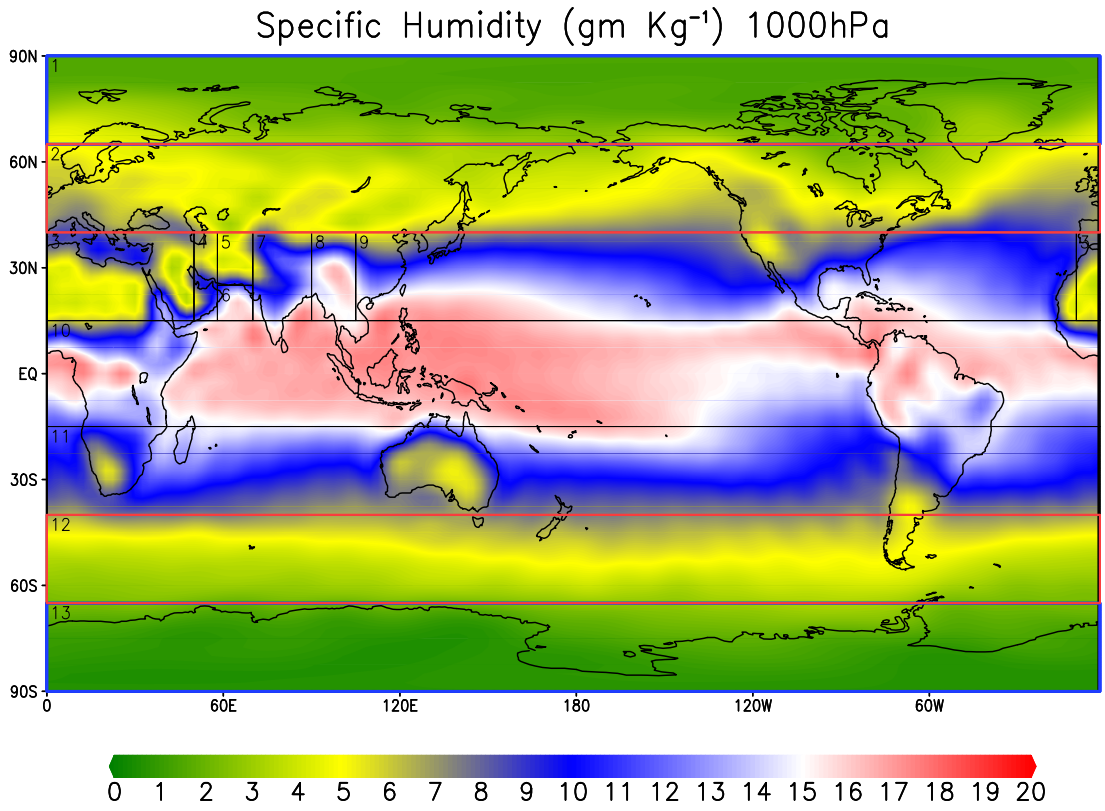

Figure 2. Long term mean of specific humidity at the surface (computed from Climate Forecast System Reanalyses product). Surface Basis Functions. Cumulus congestus profile in Red; Deep Cumulus profile in Blue; and Stratiform profile in Yellow.

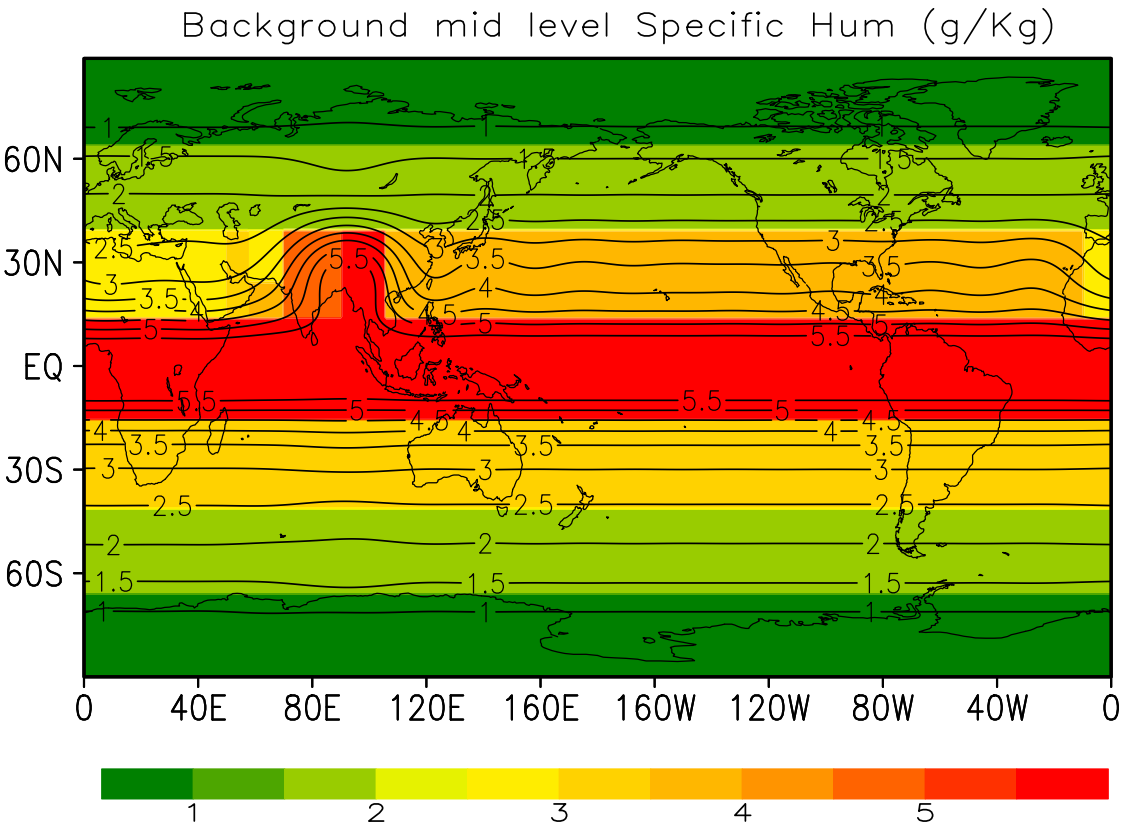

Figure 3. Background mid level Specific Humidity (g/Kg). In shading is the non-smoothed box-wise values. Smoothed field for the same is shown by the overlaid contours.

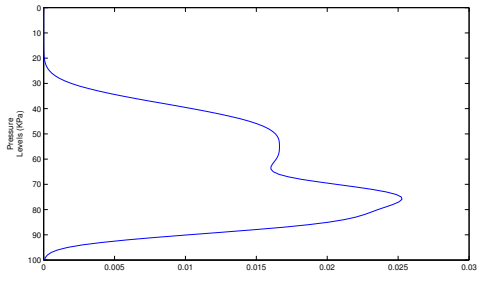

Figure 4. Q2 Profile (Drying).

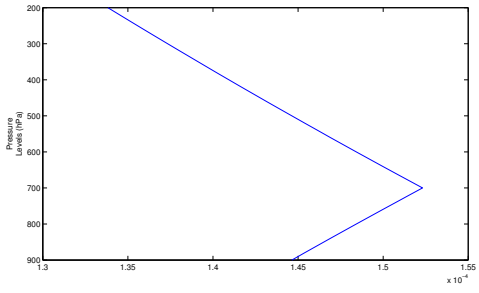

Figure 5. $\delta_m(z)$ Profile (Moistening).

The expressions of $P(z)$ and $E(z)$ ensures that, the vertically averaged convective heating balances the total amount of precipitation reaching the ground while evaporation in the free troposphere balances the drying and cooling of the PBL by downdrafts.

The temperature and moisture tendencies are computed as,

$$\left(\frac{d\theta}{dt}\right)_{conv} = Q_{tot}(z) - D_{b\theta} \tag{13}$$

$$\left(\frac{dq}{dt}\right)_{conv} = -P(z) + E(Z) - D_{bq} \tag{14}$$

Where, $D_{b\theta}$ and D_{bq} results in cooling and drying due to downdrafts below the PBL (h, which is inputted from CFS to SMCM), given by:

$$D_{bq}(z) = \begin{cases} \frac{D_c}{h}\triangle_m q & \text{if } z < h, \text{ results drying} \\ 0 & \text{if } z > h \end{cases}$$

$$D_{b\theta}(z) = \begin{cases} \frac{D_c}{h}\triangle_m \theta & \text{if } z < h, \text{ results cooling} \\ 0 & \text{if } z > h \end{cases}$$

References

Deng, Q., B. Khouider, and A. J. Majda (2015), The MJO in a Coarse-Resolution GCM with a Stochastic Multicloud Parameterization, *J. Atmos. Sci.*, *72*(1), 55–74, doi: 10.1175/JAS-D-14-0120.1.

Kasahara, A., and K. Puri (1981), Spectral representation of three-dimensional global data by expansion in normal mode functions, *Monthly Weather Review*, *109*(1), 37–51, doi: 10.1175/1520-0493(1981)109<0037:SROTDG>2.0.CO;2.

Khouider, B., and A. J. Majda (2006), A simple multicloud parameterization for convectively coupled tropical waves. part i: Linear analysis, *Journal of the Atmospheric Sciences*, *63*(4), 1308–1323, doi:10.1175/JAS3677.1.

Khouider, B., and A. J. Majda (2008), Multicloud models for organized tropical convection: Enhanced congestus heating, *Journal of the Atmospheric Sciences*, *65*(3), 895–914, doi:10.1175/2007JAS2408.1.

Khouider, B., J. Biello, and A. J. Majda (2010), A stochastic multicloud model for tropical convection, *Commun. Math. Sci.*, *8*(1), 187–216.

Khouider, B., A. St-Cyr, A. J. Majda, and J. Tribbia (2011), The mjo and convectively coupled waves in a coarse-resolution gcm with a simple multicloud parameterization, *Journal of the Atmospheric Sciences*, *68*(2), 240–264, doi:10.1175/2010JAS3443.1.

Schumacher, C., M. H. Zhang, and P. E. Ciesielski (2007), Heating structures of the trmm field campaigns, *Journal of the Atmospheric Sciences*, *64*(7), 2593–2610, doi: 10.1175/JAS3938.1.

Stachnik, J. P., C. Schumacher, and P. E. Ciesielski (2013), Total heating characteristics of the isccp tropical and subtropical cloud regimes, *Journal of Climate*, *26*(18), 7097–7116, doi:10.1175/JCLI-D-12-00673.1.

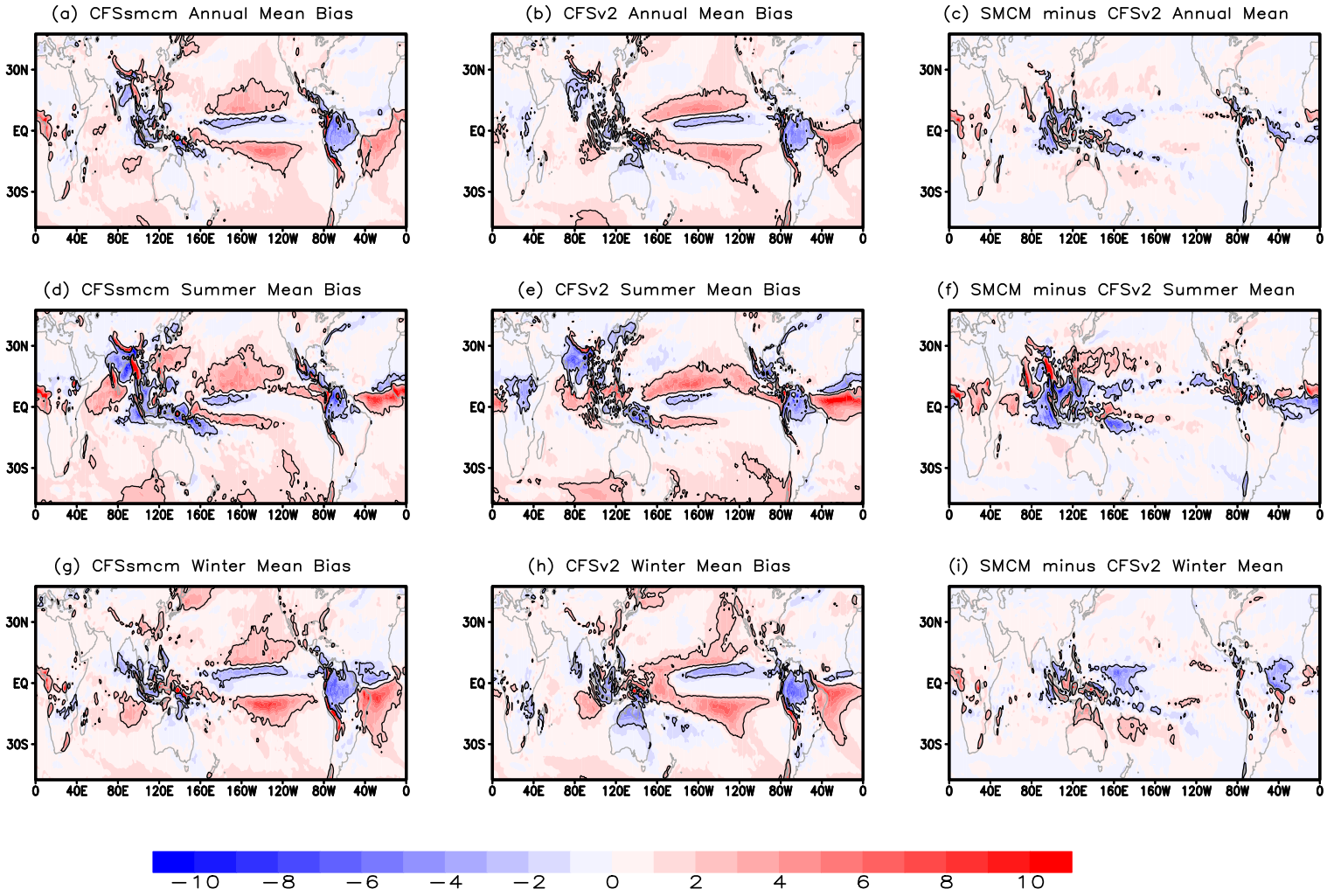

Figure 6. **(Figure S1)** Rainfall bias (mm day^{-1}) with respect to TRMM data for annual mean rainfall (a) CFSsmcm and (b) CFSv2; boreal summer mean rainfall (d) CFSsmcm and (e) CFSv2; winter (October-March) mean rainfall (g) CFSsmcm and (h) CFSv2. The difference of rainfall between CFSsmcm and CFSv2 (CFSsmcm - CFSv2) is shown in (c) Annual mean, (f) Boreal summer mean and (i) Winter mean. [The contours indicate 99% significance level]

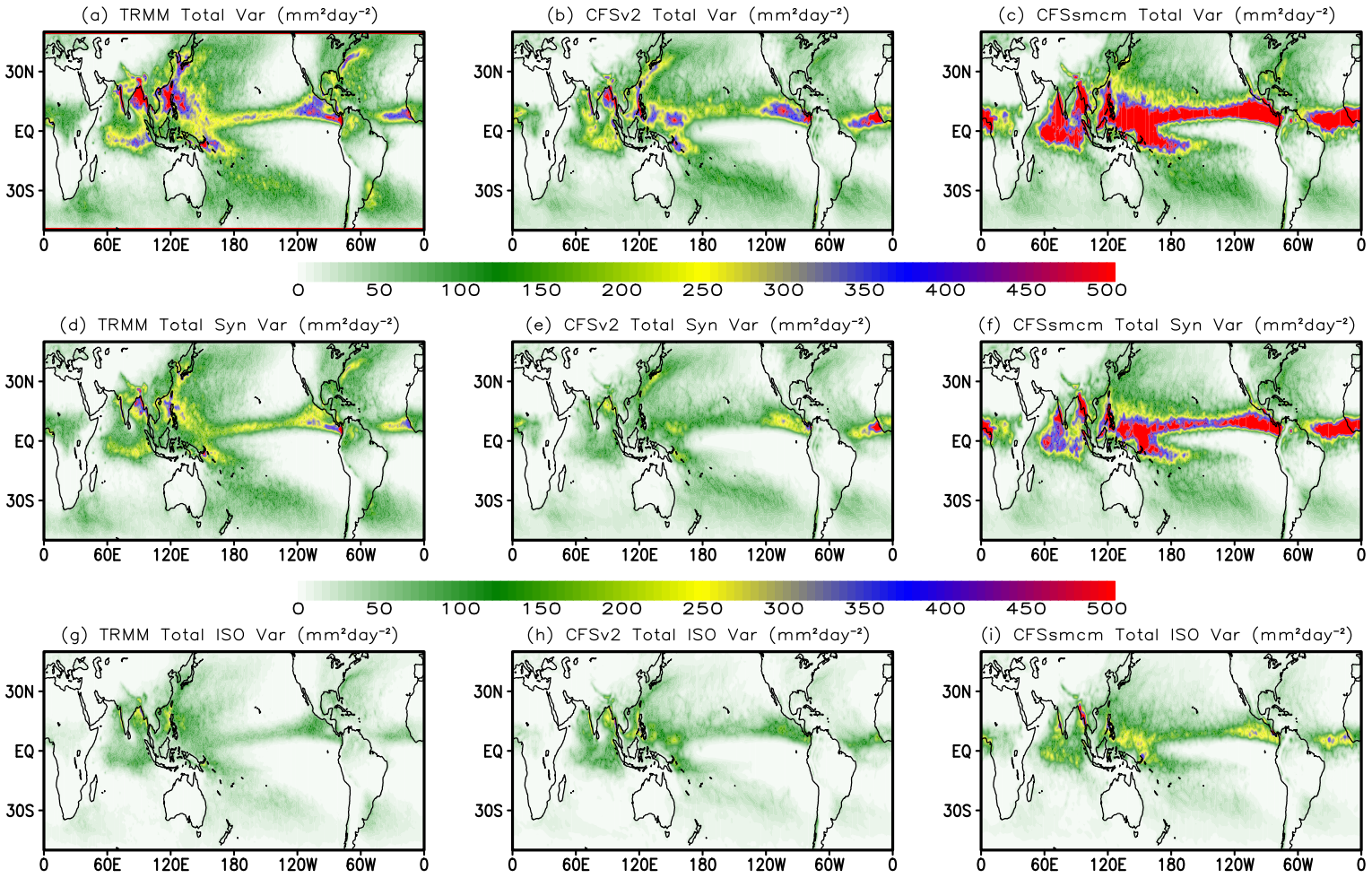

Figure 7. **(Figure S2)** Boreal summer total daily rainfall variance (a)TRMM, (b)CFSv2 and (c)CFSsmcm. Total synoptic variance (d)TRMM, (e)CFSv2 and (f)CFSsmcm. Total ISO variance (g)TRMM, (h)CFSv2 and (i)CFSsmcm.